Neuroelectronic Interfacing With Cultured Multielectrode Arrays Toward a Cultured Probe

WIM RUTTEN, JEAN-MARIE MOUVEROUX, JAN BUITENWEG, CISKA HEIDA, TEUN RUARDIJ, ENRICO MARANI, AND EGBERT LAKKE

Invited Paper

Efficient and selective electrical stimulation and recording of neural activity in peripheral, spinal, or central pathways requires multielectrode arrays at micrometer scale. At present, wire arrays in brain, flexible linear arrays in the cochlea and cuff arrays around nerve trunks are in experimental and/or clinical use. Two- and three-dimensional brush-like arrays and sieve arrays, with around 100 electrode sites, have been proposed, fabricated in microtechnology, and/or tested in a number of labs.

As there are no "blueprints" for the exact positions of neurons, an insertable multielectrode has to be designed in a redundant way. Even then, the efficiency of a multielectrode will be less than 100%, as not every electrode will contact a neural axon or soma.

Therefore, "cultured probe" devices are being developed, i.e., cell-cultured planar multielectrode arrays (MEAs). They may enhance efficiency and selectivity because neural cells have been grown over and around each electrode site as electrode-specific local networks. If, after implantation, collateral sprouts branch from a motor fiber (ventral horn area) and if they can be guided and contacted to each "host" network, a very selective and efficient interface will result.

Four basic aspects of the design and development of a cultured probe, coated with rat cortical or dorsal root ganglion neurons, are described. First, the importance of optimization of the cell-electrode contact is presented. It turns out that impedance spectroscopy, and detailed modeling of the electrode-cell interface, is a very helpful technique, which shows whether a cell is covering an electrode and how strong the sealing is. Second, the dielectrophoretic trapping method directs cells efficiently to desired spots on the substrate, and cells remain viable after the treatment. The number of cells trapped is dependent on the electric field parameters and the occurrence of a secondary force, a fluid flow (as a result of field-induced heating). It was found that the viability of trapped cortical cells was not influenced by the electric field (3 V_{pp}, 14 MHz). Third, cells must adhere to the surface of the substrate and form networks, which are locally confined, to one electrode site. For that, chemical modification of the substrate and electrode areas with various coatings, such as polyethyleneimine (PEI) and fluorocarbon monolayers promotes or inhibits adhesion of cells. The optimal diameter of local circular neurophilic areas and the separation distance between them has been investigated. Good results are obtained on wells with a diameter of 150 μm and a separation distance of 90 μm between the wells. Finally, it is shown how PEI patterning, by a stamping technique, successfully guides outgrowth of collaterals from a neonatal rat lumbar spinal cord explant, after six days in culture.

Keywords*—Cell adhesion, cell containment, collateral sprouting, cultured neurons, electrical stimulation, microfabrication, multielectrode arrays, neural engineering, neuroelectronic interfaces, neurotechnology, peripheral nerve stimulation, selectivity.*

I. INTRODUCTION

Artificial electrical stimulation of lost or impaired function, sensory or muscular, is an important tool in rehabilitation. Examples of successful clinical applications are the cardiac pacemaker and the cochlear implant. They have in common that a limited set of electrodes is sufficient to restore function of the heart (one electrode), establish some form (after intensive training) of improved understanding of speech (16 electrodes) [1] or to make use of a set of visual phosphene patterns (four electrodes) [2].

For future rehabilitative applications like graded neuromuscular control of extremities (spinal cord lesion patients), or for prosthetic vision the availability of large-scale (many electrode sites), selective neuroelectronic interface devices is one of the essential prerequisites.

In case of motor application, selective stimulation means that single motor fibers are activated, to control single muscle units, thereby enabling graded control of muscle force and the postponement of muscular fatigue. In case

Manuscript received October 1, 2000; revised February 1, 2001.

W. Rutten, J. Buitenweg, C. Heida, and T. Ruardij are with the Biomedical Engineering Department/ Faculty of Electrical Engineering/Institute for BioMedical Technology, University of Twente, 7500AE Enschede, The Netherlands (e-mail: rtn@el.utwente.nl).

J.-M. Mouveroux and E. Lakke are with the Neuroregulation, Department of Neurosurgery, Leiden University Medical Centre, 2300 RC, Leiden, The Netherlands.

E. Marani is with the Biomedical Engineering Department/ Faculty of Electrical Engineering/Institute for BioMedical Technology, University of Twente, 7500AE Enschede, The Netherlands and also with the Neuroregulation, Department of Neurosurgery, Leiden University Medical Centre, 2300 RC, Leiden, The Netherlands.

Publisher Item Identifier S 0018-9219(01)05406-8.

Table 1
Summary of Efficiencies E and E' in Eight Experiments

Experiment	E	E'	N_{el}
a	0.80	1	5
b	0.40	0.80	5
c	0.60	0.80	5
d	0.42	0.79	24
e	0.50	0.88	8
f	0.47	0.71	17
g	0.46	0.83	24
h	0.21	0.64	14
Average	0.48	0.81	

Efficiency E is defined as the fraction of the number of electrodes, which produce distinct force levels at threshold, implying that these electrodes control a separate muscle unit. If more than one electrode has the same threshold force level, only one counts, as it is assumed that this electrode contacts the same axon going to the same muscle unit. This multiple control is likely for neighbor electrodes, but less likely for electrodes that lie farther apart in the array. They will probably control another muscle unit, with an identical force. When these latter electrodes are allowed to be counted, the greater efficiency E' results. N_{el} is the number of electrodes used in an array.

of vision, being able to contact an appreciable number of optical nerve fibers selectively might restore vision partially after a long period of retraining to interpret phosphene patterns.

Artificial electrical stimulation of a nerve fiber requires a local depolarization of the axonal or somatic membrane, by a cathodic short pulse, to initiate an action potential (a 100-μs, 5-μA pulse is sufficient).

Selective stimulation means ideally a one-to-one contact between an electrode and a nerve fiber, implying that one has to limit the current spread in the endoneural tissue. Therefore, selective stimulation of nerve fibers requires a local approach of a fiber, preferably at nodes of Ranvier, the "hot spots" of (myelinated) fibers, by a microelectrode.

The electrodes should have dimensions at the scale of fiber diameters and of the widths of nodes of Ranvier, i.e., in the micrometer range. As the number of motor fibers in an average fascicle is in the order of a few hundred and the architecture of a fascicle is not precisely prescribed by nature, it is evident that currently the best possible approach present is to employ the possibilities of microfabrication techniques for the design and construction of many, preferably even a *redundant* number, of microelectrodes in two-dimensional (2-D) and three-dimensional (3-D) arrays.

In previous work [3]–[5], in the neuromuscular system, force *recruitment* experiments with a 2-D 24-fold multielectrode inside the rat peroneal nerve resulted in *selective* stimulation of motor fibers with an average efficiency of 48% (this means about 12 of 24 electrodes control a different muscle unit); see Table 1 and Fig. 1. These experiments (and previous experiments with a linear array [6]–[10]) guided the design and fabrication of the University of Twente 3-D 128-fold silicon microelectrode device. Alternatively, fabrication of a 2-D 128-fold multielectrode device in LIGA technology was performed (Fig. 2) [11].

A recent example of a 3-D device is the stacked multielectrode system of the Michigan group [12]. Other approaches

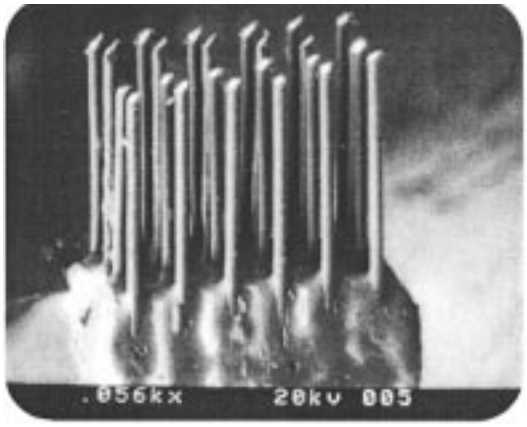

Fig. 1. Micrograph of 24-fold 2-D electrode array. Electrode spacing is 120 μm.

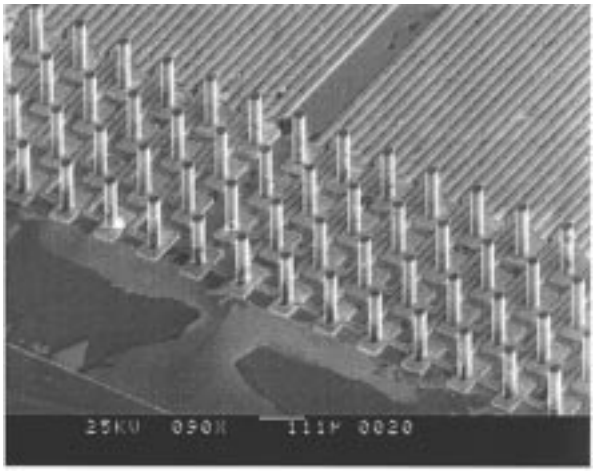

Fig. 2. Multielectrode array with 150-μm-tall 20-μm-diameter nickel needles, realized with aligned X-ray lithography (LIGA) on silicon substrate with 8-μm Cu interconnection wiring. Interdistance is 120 μm.

are the sieve-regeneration types of interface in which fibers grow through via holes or slits in 2-D "neural sieve" multielectrodes, the number of contact sites being limited to at most 12 [13], [14].

A. Cultured Multielectrode Arrays as Efficient Neuroelectronic Interfaces

As nature provides no "blueprints" for the exact positions of neurons, an insertable multielectrode has to be designed in a redundant way, implying that the efficiency of a multielectrode will be less than 100%. Therefore, it is investigated how in-vitro-neuron cell-cultured microelectrode arrays (MEAs) might enhance efficiency after implantation as hybrid prosthetic devices. In these so-called "cultured probe" devices, neural cells have been grown on electrode substrates in a way that a group of cells belongs exclusively to one electrode site, i.e., an electrode-specific local network. If, from the in-vivo side, after implantation, collateral sprouts branch from a motor fiber (ventral horn area) and can be guided and contacted to each host network, a very selective and efficient interface will be the result (Fig. 3).

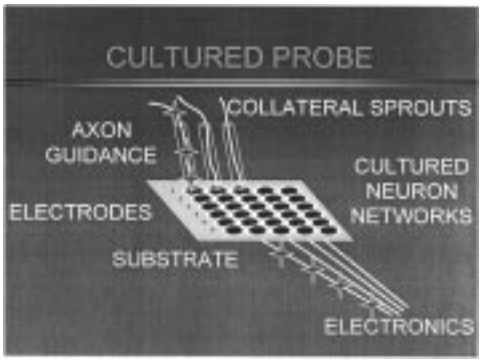

Fig. 3. Schematic impression of a "cultured probe" neural prosthetic device. Important aspects are: 1) cell–electrode adhesion; 2) trapping of cells; 3) adhesion of local neural networks; and 4) sprouting of collateral fibers.

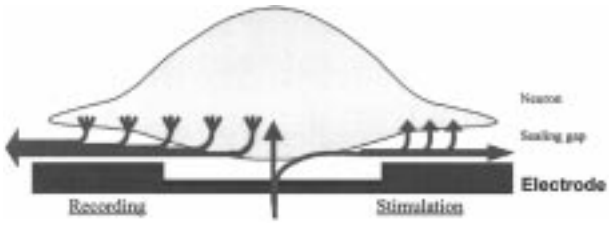

Fig. 4. Effect of complete sealing on the neuron–electrode contact. Currents from the lower membrane or from the electrode will produce a potential field in the sealing gap, which mediates in extracellular recording and stimulation.

The remainder of this paper presents the following topics.

- It is shown how *cell-electrode impedance* measurement indicates quality of cell-substrate adhesion.
- Also, *trapping of cells by dielectrophoretic forces*, and their viability, is demonstrated.
- Furthermore, improvement and understanding of *adhesion of isolated local networks of neurons* is described
- Finally, it is shown how *sprouting collateral fibers* grow out from a cultured network and can be guided toward electrodes.

II. Cell–Electrode Impedance

A. Tools for Studying the Neuron–Electrode Contact

The efficiency of a cultured probe will depend on the quality of the individual electrical contacts between the microelectrodes of the device and the neurons in the culture. High-quality neuron–electrode contacts will permit very selective stimulation of and reliable recording from a single neuron or a small group of neurons.

Experimental results, reported in literature, indicate that the quality of the neuron–electrode contact improves when the electrode is completely covered, or sealed, by the neuron [16]–[18]. In Fig. 4, the effect of complete sealing is illustrated. In case of stimulation, the current arising from the electrode will produce a potential field in the sealing gap, which can induce a current through the lower membrane. In case of recording, the current in the sealing gap will arise from the lower neural membrane and the resulting potential field is measured with the electrode. The magnitude of this field is proportional to the resistance of the sealing gap and, therefore, the sealing resistance is an important factor in the neuron–electrode contact.

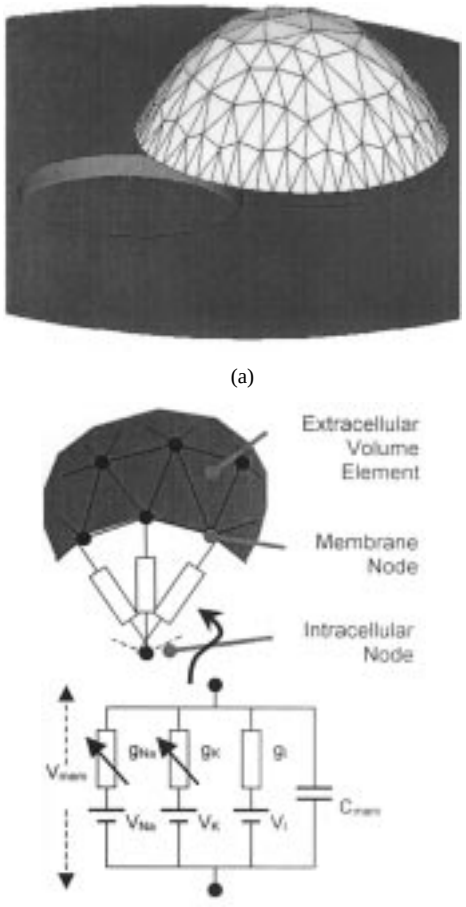

Fig. 5. (a) 3-D visualization of the neuron–electrode interface geometry, as implemented in the finite element model. (b) The neuronal membrane is represented by a set by dynamic circuit elements, connecting the extracellular and intracellular membrane nodes. These circuit elements are defined with Hodgkin–Huxley-like properties.

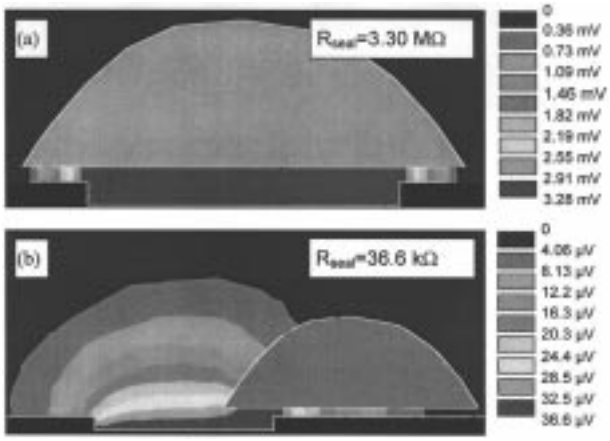

Fig. 6. Computed potentials due to a 1-nA stimulus current through the microelectrode in a cross section of the model. The equipotential lines are marked by the boundaries between two colored regions.

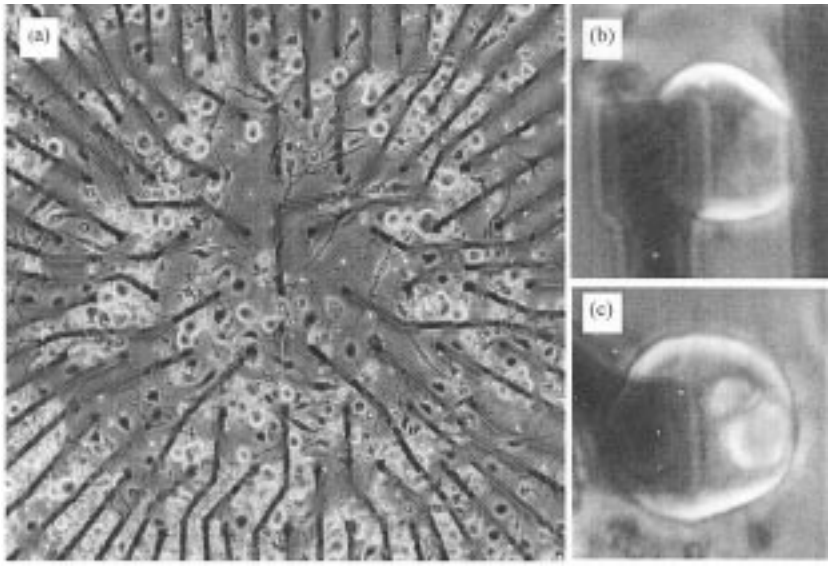

Fig. 7. (a) Multielectrode array with a purified culture of DRG neurons from neonatal rats after 1 DIV. (b) DRG neuron partially covering an electrode. (c) Complete coverage of an electrode by a DRG neuron.

The effect of complete sealing demonstrates that the electrical properties of the neuron–electrode interface are related to its geometry, i.e., size, shape, and mutual position of neuron and electrode. For understanding and optimization of the neuron–electrode contact, we need experimental as well as theoretical tools to study these electrical properties.

B. Theoretical Tool

To study the neuron–electrode contact on a physical basis, the finite element method is applied for modeling the electrical behavior of the neuron–electrode interface [19], [20]. This method permits numerical solutions of volume conductor problems for a variety of geometries. In Fig. 5, a visualization of the model is depicted for a parametrical geometry. A circular neuron with a parabolic height profile is positioned on top of a circular electrode. Below the neuron, the sealing gap is modeled. In this figure, the neuron is shifted off the electrode but the sealing can be made complete by decreasing the eccentricity of the neuron. The entire extracellular space is meshed with volume conductor elements (not shown). The neural membrane is modeled with dynamical circuit elements, which resemble Hodgkin–Huxley-like electrical behavior. These circuit elements connect the nodes on the extracellular surface of the neuron with a single intracellular node. Both intracellular and extracellular current stimulation can be applied and the electrode potential, local membrane potentials, and current densities can be computed.

As an example, the consequences of complete and incomplete sealing are presented in Fig. 6 for a neuron with a diameter of 14 μm and an electrode with a diameter of 10 μm. The computed potential field due to a 1–nA stimulus current through the electrode is depicted in a cross section of the model. The equipotential lines in the medium are marked by the boundaries between regions with different colors. At complete sealing [Fig. 6(a)], these equipotential lines are concentrated in the sealing gap, indicating the potential field in the sealing gap. This potential field induces a maximum depolarization of 1.02 mV at the upper membrane and a hyperpolarization of 2.25 mV occurs at the lower membrane. When the sealing is incomplete [Fig. 6(b)], the equipotential lines are spread up more widely, indicating a leakage current into the medium. The changes in membrane potential are reduced to the microvolt range. At complete sealing, a sealing resistance is computed of 3.28 MΩ and at incomplete sealing, a spreading resistance of only 36.6 kΩ remains.

C. Experimental Tool

A proper experimental setup for studying the neuron–electrode contact should provide neuron–electrode interfaces in a range from partial to complete electrode coverage with sufficient extracellular and intracellular electrical accessibility. Furthermore, the geometry of the interface should be observable, in order to link the electrical measurements to the theoretical model.

To meet these requirements, MEAs were used to obtain electrical contacts with cultured neurons. The MEAs consist of 61 electrodes with diameter of 5 and 10 μm, organized in a hexagonal array with a distance of 80 μm between the centers of two adjacent electrodes [Fig. 7(a)]. The electrode tips are covered with titanium nitride, resulting in a very low electrode-electrolyte impedance to improve extracellular electrical accessibility ($<$300 kΩ at 1 kHz). Unfortunately, these impedances will increase during the culturing period due to pollution of the electrodes with cell debris (typical impedances around 500 kΩ).

On the MEAs, cells from dissociated neonatal rat dorsal root ganglions (DRG) are cultured. DRG neurons have a typical diameter of 30 μm, which is relatively large when compared to other neurons of the nervous system, such as cortical or hippocampal neurons. Hence, these neurons can easily cover a microelectrode completely. A purification protocol

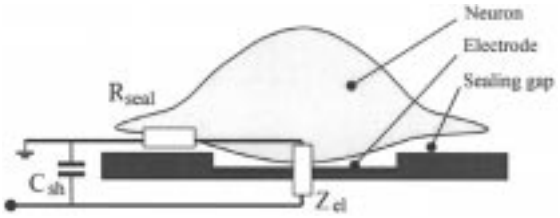

Fig. 8. Impedance model of the neuron–electrode interface for interpretation of measured impedance.

is applied to increase the neural content of the culture from 5% up to 30%. Furthermore, R12 medium [101] is used to suppress proliferation of nonneural cells. Due to this method, cultures are obtained with increased probability of complete electrode coverage and low aggregation of neurons by nonneural cells. As a result, the geometry of neuron–electrode interfaces is observable during several days in vitro [Fig. 4(b) and (c)].

Since the resistance of the sealing gap is such an important factor in the neuron–electrode contact, a method is developed to determine the sealing resistance from the impedance spectrum of the total neuron–electrode interface. In previous work, it is demonstrated that this impedance spectrum depends on the impedance of the electrode, the resistance of the sealing gap and on the shunt capacity between the electrode wire and the medium (over the insulation layer) [21]. The impedance spectrum is not sensitive to the relatively high impedance of the neural membrane (Fig. 8). Fig. 9(a) illustrates how the impedance spectrum of the neuron–electrode interface is formed by the properties of the electrode, the sealing resistance and the shunt capacity. Presentation of the spectrum as an impedance locus permits easy evaluation of the electrode impedance and sealing resistance at first sight. More precise analysis can be performed by fitting the parameters of the impedance model to the locus.

As a demonstration of electrical accessibility, the impedance spectra are depicted, which were measured at several moments during an experiment [Fig. 9(b)]. The first impedance locus was measured at the start of the experiment, before culturing. The second locus was measured after 5 h in vitro: a neuron was covering the electrode partially. The next day, this neuron had covered the electrode (almost) completely. After this measurement, the neuron was removed from the electrode with a glass pipette and the impedance locus was measured again.

D. Coupling Theory and Experiment

The finite element method permits modeling of almost any geometry and is not restricted to parametrical geometries, as defined above. Therefore, more realistic shapes of neurons can be modeled easily which is very advantageous when it comes to experimental characterization of the electrical properties of the neuron–electrode interface.

As an illustration, the neuron–electrode interface from Fig. 7(b) is used for reconstruction of the interface geometry. The circumference of neural soma and electrode are marked on a digitized microphotograph. From these countours, the geometries are reconstructed [Fig. 10(a)]. The assumption of a parabolic height profile is applied again, since the above presented simulations revealed that the influence of height was not very large. The maximum height is taken a quarter of the maximal diameter of the neuron.

Based on the reconstructed geometry, mesh generation is performed. A stimulus current is applied through the electrode and the initial membrane potentials are computed. In Fig. 10(b), the membrane potential distribution is depicted on the model that is superimposed on an image of the electrode. A view, from below, in Fig. 10(c), reveals that most of the membrane polarization is localized at the site of electrode and in the sealing gap. The computed potentials can be related directly to experimentally derived potentials of the electrode and the intracellular space which permit identification of the electrical properties of the neuron–electrode interface.

III. Trapping of Cells by Dielectrophoretic Forces

Negative dielectrophoretic trapping of neural cells is an efficient way to position neural cells on the electrode sites of planar microelectrode arrays. Dielectrophoresis (DEP) is the creation of forces on neutral, but polarizable particles in nonuniform electric fields [22], [23]. The time-averaged dielectrophoretic force F_{DEP} exerted on a particle p suspended in a medium m exposed to an alternating current (AC) electric field depends on is dependent on the in-phase component of the dipole moment, and can be expressed as

$$\vec{F}_{\mathrm{DEP}}(\omega,x,y,z) = 2\pi r^3 \varepsilon_m \mathrm{Re}\left[\frac{\varepsilon_p^*(\omega)-\varepsilon_m^*(\omega)}{\varepsilon_p^*(\omega)+2\varepsilon_m^*(\omega)}\right] \times \nabla \vec{E}^2_{\mathrm{rms}}(x,y,z) \quad (1)$$

where the index rms denotes the root-mean-square value of the electric field, $\omega = 2\pi f$ with f the frequency of the electric field, r is the radius of the particle, and ε^* is the complex permittivity

$$\varepsilon^*(\omega) = \varepsilon - j\frac{\sigma}{\omega} \quad (2)$$

where $j = (-1)^{1/2}$, ε and σ are the permittivity and conductivity, respectively. According to (1), the DEP force is a function of the dimension of the particle, the electrical properties of particle and medium, and the distribution of the electric field. The electrical properties of particle and medium are included in the so-called *Clausius-Mosotti factor* (f_{CM})

$$f_{\mathrm{CM}}(\omega) = \frac{\varepsilon_p^*(\omega)-\varepsilon_m^*(\omega)}{\varepsilon_p^*(\omega)+2\varepsilon_m^*(\omega)}. \quad (3)$$

The real part of this factor gives the frequency dependence and the direction of the dielectrophoretic force (1). For medium with a conductivity of 1 S/m or more negative dielectrophoretic forces, i.e., forces that direct the particle away from the electrodes, are created over a wide frequency range [24]. Therefore, a quadrupole electrode configuration (see Fig. 11) can effectively be used to trap neurons.

Two important aspects with respect to the dielectrophoretic trapping procedure are the number of cells that can be trapped at a particular spot under certain field

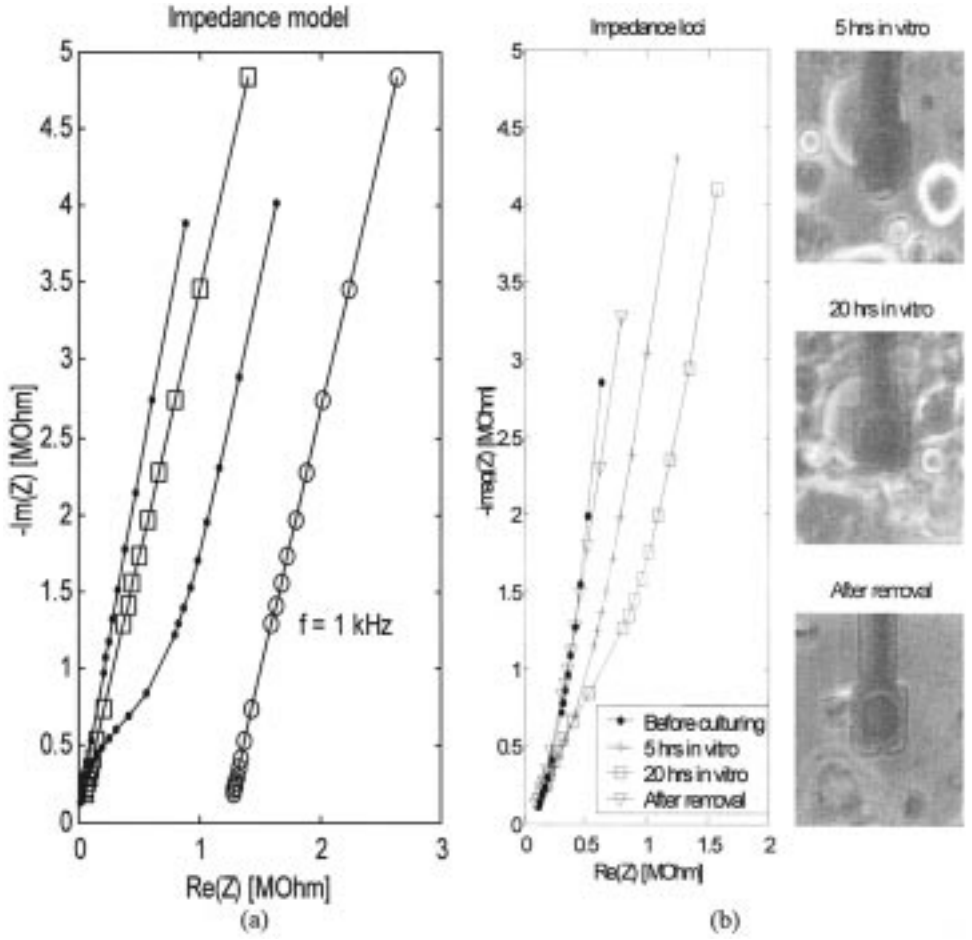

Fig. 9. (a) Modeled impedance loci of the electrode–electrolyte junction $Z_e = K/(i \cdot 2 \cdot \pi \cdot f)$ alone (•) and in series with a sealing resistance $R_{\text{seal}} = 1.2\ \text{M}\Omega$ (□). On a MEA, these impedane loci are in parallel with the shunt capacity (•); see, also, Fig. 8. (b) Measured impedance loci from cultured neuron–electrode interfaces. The changes in the impedance loci are caused by coverage of the electrode by the neuron.

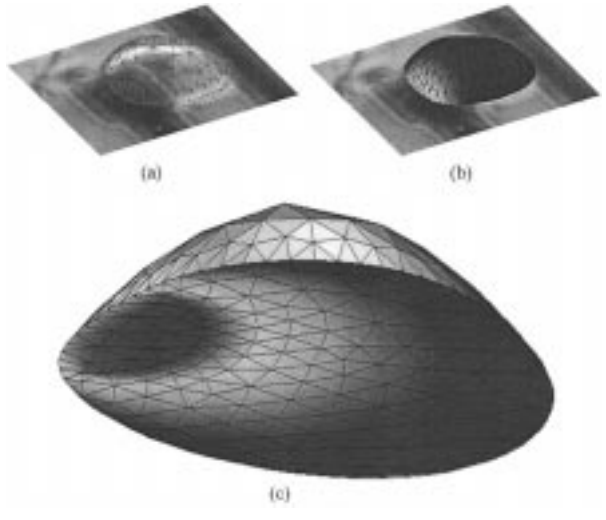

Fig. 10. Modeling of neuron–electrode interfaces using geometry reconstruction from microphotographs. The pseudocolors mark the potential distribution over the membrane.

conditions and the viability of the cells after being exposed to the electric fields.

A. Quantitative Aspect of DEP Trapping

Dielectrophoretic trapping of particles of micrometer dimensions requires field strengths between two and several hundred kilovolts/m [25]–[27]. With an interelectrode distance of 100 μm and amplitudes of several volts, these field strengths can easily be obtained. However, due to the frequency dependent electric properties of cells and medium different numbers of cells are trapped using different amplitude and frequency combinations. Fig. 12 shows an example of cortical cells of postnatal day two trapped in the center of a quadrupole electrode structure.

Experiments showed that embryonic as well as postnatal cortical rat cells could be trapped using sinusoidal input signals of 1–5 V_{ptp} and frequencies in the range from 10 kHz to 50 MHz. Fig. 13 shows the number of embryonic cells trapped in the center of the quadrupole electrode structure for two different input signals. The field was applied for 30 min, but cells were mainly trapped during the first 20 min.

The results shown in Fig. 13 were in contradiction with the theoretical prediction. Based on a single-shell model for the neuron, the Clausius–Mosotti factor suggested that the dielectrophoretic force would decrease with increasing fre-

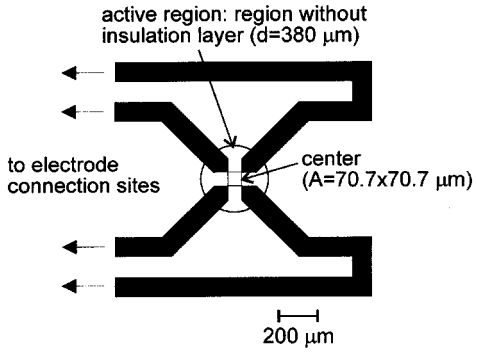

Fig. 11. Schematic diagram of the quadrupole electrode structure. A glass plate (5 × 5 cm, thickness 1 mm) was used as a substrate for the gold electrodes. The distance between two diagonally opposing electrodes is 100 μm. An insulation layer consisting of a silicone nitride layer ($\mathrm{Si}_x\mathrm{N}_y$) of 396 nm sandwiched between two layers of silicon oxide (SiO_2) of 144 nm each was deposited over the electrode plate except for the "active regions" and at the connection sites located at one of the edges of the glass plate.

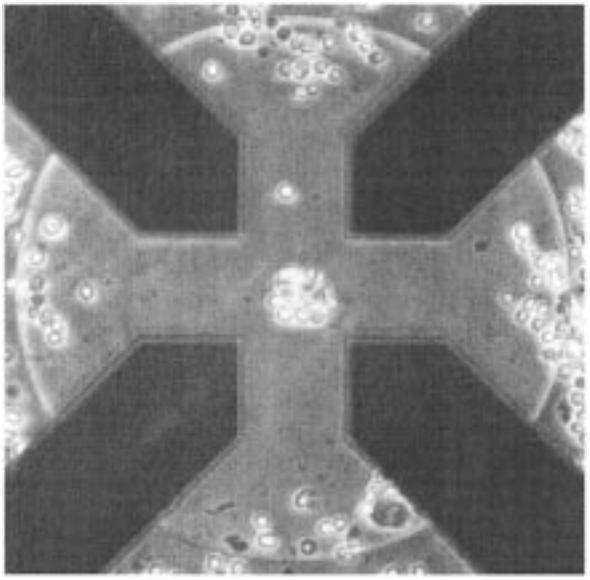

Fig. 12. A dense cluster of cortical rat cells of postnatal day two trapped in the center of the quadrupole electrode structure after 30 min of field application ($5\ \mathrm{V_{pp}}/100$ kHz). The cells have a diameter of about 10 μm.

quency. The single-shell model represents the cell a homogeneously conducting sphere surrounded by a membrane acting as a capacitor [28]–[30]. By gradually decreasing the DEP force, it was expected that the situation would resemble the situation in which no field was present more and more. However, even at high frequencies a dense cluster of cells, as shown in Fig. 12, was trapped in the center. Therefore, besides the dielectrophoretic force a secondary force is responsible for the trapping process. This force is dependent on the input signal.

Due to the high conductivity of the medium, the presence of an electric field results in heating of the medium. This local heating gives rise to a fluid flow. The maximum temperature rise in the center of the structure was measured to be 1.2° C for an amplitude of 5 V and 0.6° C for an amplitude of 3 V. In both cases, the frequency was 50 MHz. Due to the configuration of the electrodes, this flow enhances the trapping effect [27], [31], [32]. It was most apparent for large input signals of high frequencies, which explains the results shown in Fig. 13 for frequencies above 4 MHz.

B. The Qualitative Aspect of DEP Trapping

When using dielectrophoretically trapped neurons for recording and stimulation purposes a prerequisite is that the neurons are still viable after being exposed to the nonuniform electric fields. High field strengths may lead to excessive membrane potentials. A membrane potential of 1 V for even a short duration was found to result in the formation of pores in the membrane [33]. This was found for several eukaryotic cells (e.g., mouse L-cells, mouse myeloma cells, human erythrocytes), but never for neurons.

Obtaining the membrane breakdown potential includes methods like studying the breakdown-induced uptake or release of radioactive isotopes or of other indicator substances in response to an external field, recording membrane potential changes with voltage-sensitive fluorescent dyes, or the use of patch clamp techniques [33]. Once the critical field strength is known, the membrane potential at which breakdown occurs can be calculated. The values of the membrane breakdown voltage of the cells mentioned above were determined under the assumption that the cell can be represented by a single-shell model, the electric field is uniform, the resting membrane potential is not changed by the external field, the generated membrane potential is superimposed linearly upon the resting membrane potential, and surface admittance and space charge effects do not play a role [33].

The occurrence of membrane breakdown is, however, unpredictable in the case of dielectrophoretically trapped neural cells. One aspect is the nonuniformity of the field, which with increasing cell density becomes even more nonuniform. This may result in the exposure of cells in the suspension to field strengths that differ considerably from that expected theoretically. Furthermore, it is still questionable if the use of a single-shell model is a legitimate representation of a neural cell (see the previous paragraph). Accordingly, the assumptions about resting and generated membrane potentials and surface admittance may not be valid for neural cells since electrical phenomena play an important role in the function of these cells. In addition, the membrane breakdown was found to decrease with increasing temperature. Local heating of the medium with rather high conductivity (> 1 S/m) due to the presence of an electric field is almost inevitable. Therefore, it is important to examine the viability of dielectrophoretically trapped cells in culture.

The viable state of postnatal cortical rat cells after field exposure ($3\ \mathrm{V_{ptp}}$, 14 MHz applied for 1 h) was compared to that of nonexposed cells with respect to the number of outgrowing and nonoutgrowing cortical cells and to outgrowth-related morphological characteristics.

The area taken up by the soma of the cells gives an indication of the adhesiveness of the cell. Since the electric field

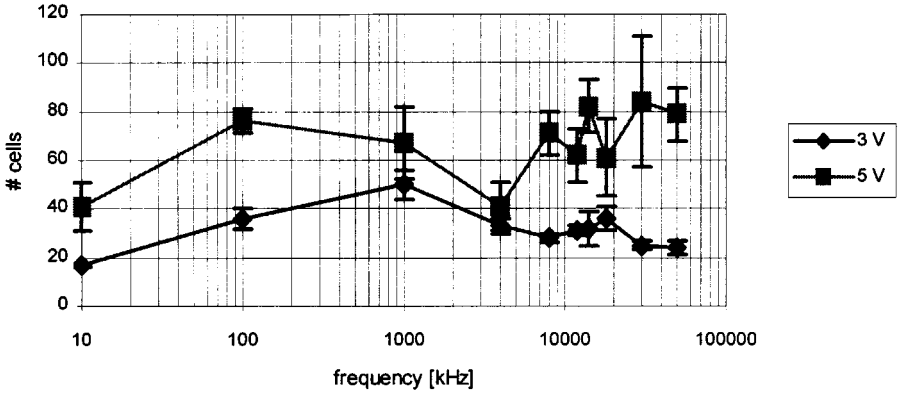

Fig. 13. The number of cells trapped in the center of the quadrupole electrode structure after 20 min of field application using two different input signals (3 and 5 V_{pp}) and frequencies ranging from 10 kHz to 50 MHz.

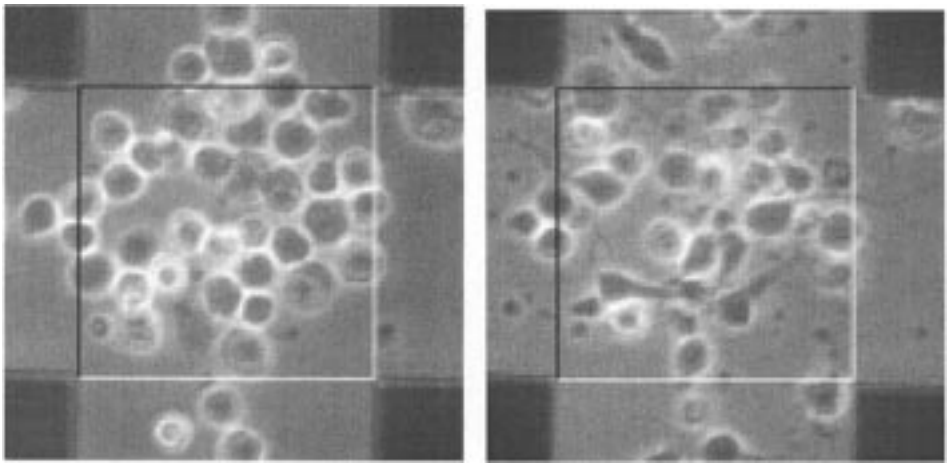

(a) (b)

Fig. 14. Postnatal cortical rat cells trapped in the center of the electrode structure 4 h after field application (a) and 1 DIV (b). The analysis with respect to the viability of the cells was restricted to the center of the electrode structure. For the control experiments, a randomly chosen square area of the same size was used. The black and white sides of the square indiate that cells were allowed to lie across two sides of the area. The processes were allowed to cross all sides of the area when orginating from cells that satisfy the previous constraint.

may influence the cell membrane, a difference in adhesiveness between exposed and nonexposed cells as compared to that of reference cells can be expected. In addition, swelling by osmotic processes may occur due to a temporary change in membrane permeability caused by the electric field. The area of cells was determined by drawing a contour around their soma and calculating the included area using the software package VIDAS (Carl Zeiss B.V., Weesp, The Netherlands). If cells adhere and grow out they are considered viable, making the number and length of the processes a direct quantitative measure for the viability of the cells. The number of cells and processes were manually counted, and the process-length was determined using VIDAS.

Fig. 14 shows the images of trapped postnatal cortical cells 4 h after field application and after one day in vitro (1 DIV). Analysis of the aspects mentioned above was performed during five days.

The results showed that the size of the cells did not change, meaning that no (temporary) membrane breakdown, resulting in osmotic processes or changes in membrane properties, had occurred. Fig. 15(a) shows the average area of a cortical cell in the trapped as well as the reference situation. In addition, no differences in the number of outgrowing processes per cell and the length of these processes were detected. Due to the dielectrophoretic trapping procedure the number of cells trapped was always larger than the number of homogeneously positioned cells in the reference situation. Taking into account this difference the data concerning the total number of cells, the number of outgrowing and nonoutgrowing cells and the number of processes was "normalized." This is shown in Fig. 15(b) for the number of processes over time for both situations. No significant differences between the trapped and reference situation were found for the normalized aspects.

In conclusion, negative dielectrophoretic trapping can be used to collect cortical rat cells at the recording and stimulation sites of a microelectrode array. The number of cells trapped depends on the field parameters used and the occurrence of a secondary force, a fluid flow as a result of field-induced heating at large input signals and high frequencies.

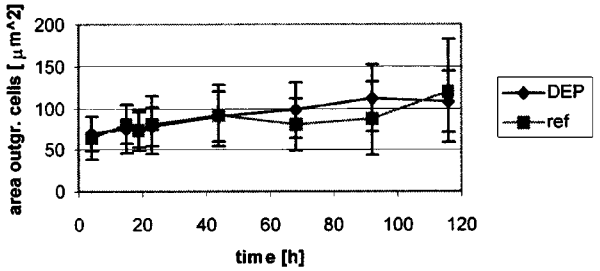

(a)

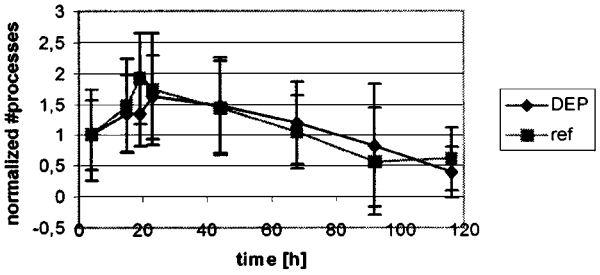

(b)

Fig. 15. (a) Average area per outgrowing cortical cell for the trapped (DEP) as well as the reference (ref) cortical cells as a function of time. (b) Normalized number of processes located within the defined area for both situations over time.

It was found that the viability of trapped cortical cells was not influenced by the electric field (3 V_{ptp}, 14 MHz). Therefore, dielectrophoretic trapping is an effective and harmless method to position cortical cells on the electrode sites of multielectrode arrays.

IV. Adhesion of Isolated Local Networks of Neurons

Local networks of neurons on microelectrodes of MEAs can be obtained by selective adhesion of dissociated neurons on top of electrodes and a subsequent containment of the outgrowing neurites and/or fascicles within a predefined area around the electrodes. Selective chemical modification of the surface of a MEA is considered as one of the gateways toward the goal of enhanced selectivity and is usually obtained with photolithography-based methods [34], [35]. A promising solution for the nonadhesive part of precultured MEAs was described by Makohliso *et al.* [36], who investigated spin-coated fluorocarbon (FC) layers as nonadhesive materials for neurons. The properties of fluorocarbon coatings resemble the properties of polytetrafluoroethylene [37], [38], a very hydrophobic biocompatible material with nonadhesive properties to cells due to irreversible adsorption of albumin [39]. On the other hand, the choice for nonspecific neuron-adhesive coatings is often driven by the supposed electrostatic interaction between positively charged amino groups (polyamines) and negatively charged phospholipids in the cell membrane [40]. A material that exploits this feature and avoids the presence of hydrolysable peptide-like amide linkages in the polymer backbone, is polyethylenimine (PEI) [41]. The combination of a nonadhesive FC coating and an adhesive PEI coating is therefore considered as a promising solution toward selective neuron adhesion and additional long-term maintenance. The subsequent containment of neurites and/or fascicles can be mediated by variation of the separation distance between the PEI-coated areas [42].

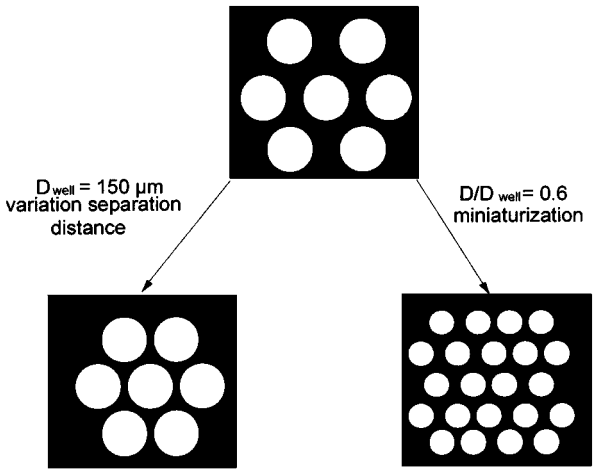

Fig. 16. Top view of the neuron adhesion experiments of PEI-coated wells. Experiments were done on a series of patterns with a fixed well-diameter (150 μm) and decreasing separation distance (left arrow) or a series of patterns with a combined variation of well-diameter and separation distance (right arrow). Black represents the FC-layer.

A. Preparation Procedure of Chemical Patterns With PEI and FC

Insufficient adhesion between glass and FC was circumvented by deposition of a sticky spin-coated polyimide (PI, Probimide 7510, Arch Chemicals N.V., Zwijndrecht, Belgium) layer[38]. FC coatings have been deposited in a reactive ion etching (RIE) system via a plasma-polymerization of carbonhydrotrifluoride (CHF_3). Samples were initially treated with an etching CHF_3/O_2, a depositing CHF_3 treatment and a second low-energy treatment in CHF_3. The FC coatings were spin-coated with a protective layer of positive photoresist (OiR 07/17, Arch Chemicals N.V.). Photoresist was selectively developed and removed from the surface (Developer OPD 4262, Arch Chemicals N.V.) after UV light exposure through a chromium mask. The underlying FC and PI layers were removed with an etching CHF_3/O_2 plasma. Finally, the adsorption of PEI (Fluka Chemie AG, Buchs, Switzerland) on the surface was done with a so-called PEI liftoff method [42]. Samples were immersed in a PEI solution (10 μg/ml). After the PEI treatment, photoresist with adsorbed PEI was removed by rinsing in a 1.0-m NaOH solution, followed by immersion and rinsing in milli-Q water (1 min).

B. Experimental Setup

In a first study, patterns of PEI-coated wells (diameter of 150 μm, depth 0.5 μm) embedded in a neuron-repellent Plasma-FC layer, were investigated. The wells were arranged on nine separate subsections of a sample with a constant separation distance between the wells within each section. Separation distances between the wells were varied from 10 μm up to 90 μm on nine different subsections of a sample

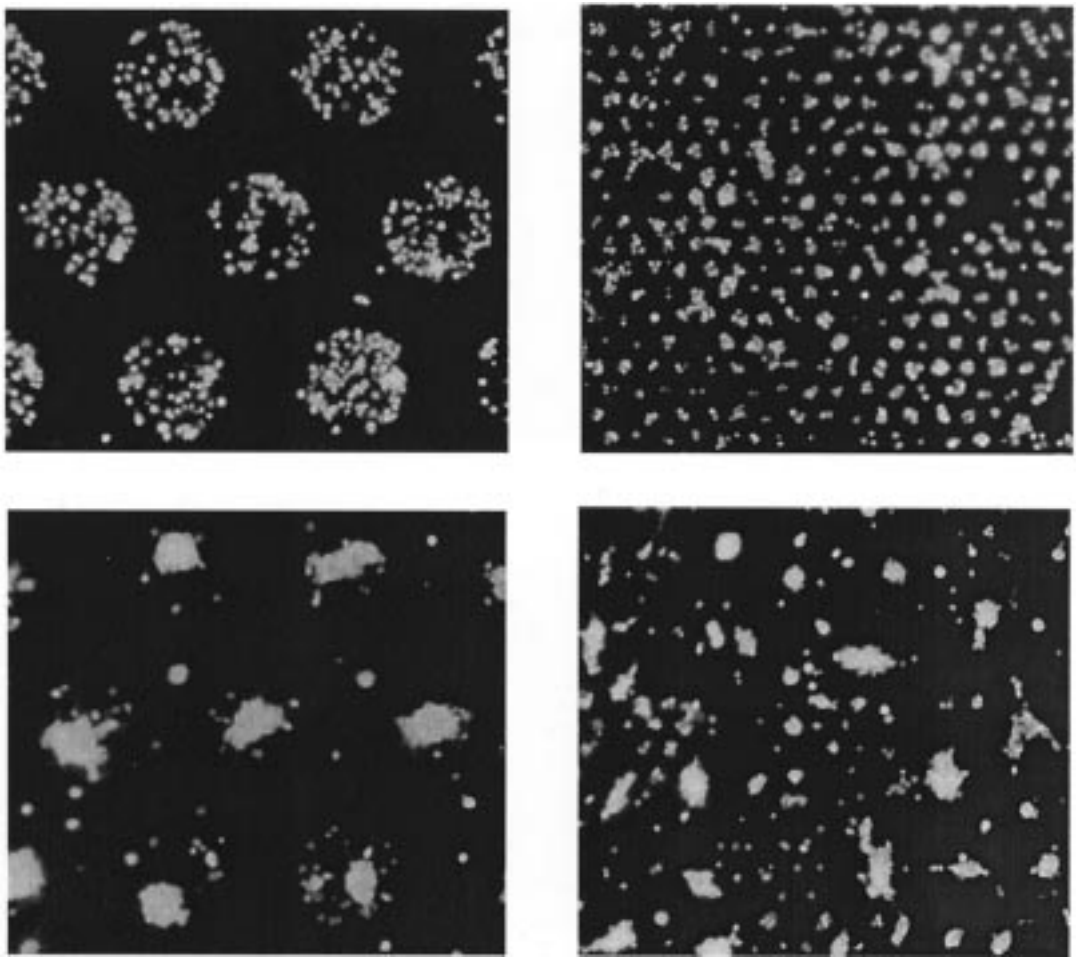

Fig. 17. Fluorescent images of acridine orange (green)-propidium iodide (red) stained cortical neurons on PEI-coated wells with a diameter of 150 μm (left) and 25 μm (right). Results are shown after one day (top) and four days (bottom) in vitro. Dark areas represent the FC layer.

(Fig. 16). In a second study, separation distances and diameters of PEI-coated wells were varied simultaneously to investigate the influence of chemical pattern miniaturization on neuron adhesion and neurite development. The distance between the wells was kept at a constant fraction (0.6) of the diameter D of the wells (Fig. 16). Four subsections of the chemical pattern were assembled on each sample. The well diameter D was 150, 100, 50, and 25μm on the four subsections mentioned. Consequently, this corresponded to separation distances of 90, 60, 30, and 15 μm between the wells.

C. Results

Cerebral cortex from 1-day-old newborn rats was dissected out under sterile circumstances and was dissociated into single neurons. Viable and nonviable neurons were also evaluated with a staining procedure using acridine orange (AO) and propidium iodide (PPI), respectively [43]. Examples of cortical neuron adhesion after one day *in vitro* are presented in Fig. 17. The results emphasize some typical phenomena observed during the miniaturization experiments. Polyethylenimine (PEI) was an excellent neurophilic coating and supported the adhesion of cortical neurons inside the PEI-coated wells to a significant extent. Approximately all of the observed neurons were located on the PEI-coated wells with a separation distance of 90 μm between the wells (diameter is 150 μm) after one day *in vitro*. Apparently, the CHF_3 plasma deposited fluorocarbon layer served as a nonadhesive coating for cortical neurons. The results on the miniaturized patterns (Fig. 2, right side) were somewhat different. Neurons preferentially adhered on 25 μm (diameter) wells although clusters of neurons were also visible on the CHF_3 layer after one day *in vitro*. This observation became even more clear after four days (Fig. 17, bottom). On the 150-μm (diameter) wells, aggregates of neurons were formed but the neural tissue was still located on the PEI-coated wells. The location of neural tissue on 25-μm wells, however, was almost random. Viability of neural tissue was assessed by the color of the tissue after cytochemical staining. The general observation is that a large number of neurons forms aggregates after active migration of the adhering neurons toward each other. The images in Fig. 18 support the hypothesis that neurons within an aggregate lose their viability. A lack of nutrition, caused by a limited diffusion of medium components toward encapsulated neurons, probably enhances cell death significantly. An important observation supporting this hypothesis is the fact that areas with yellow tissue could clearly be identified, apart from the expected red (PI-stained) and green (AO-stained) tissue. A yellow color after staining is expected

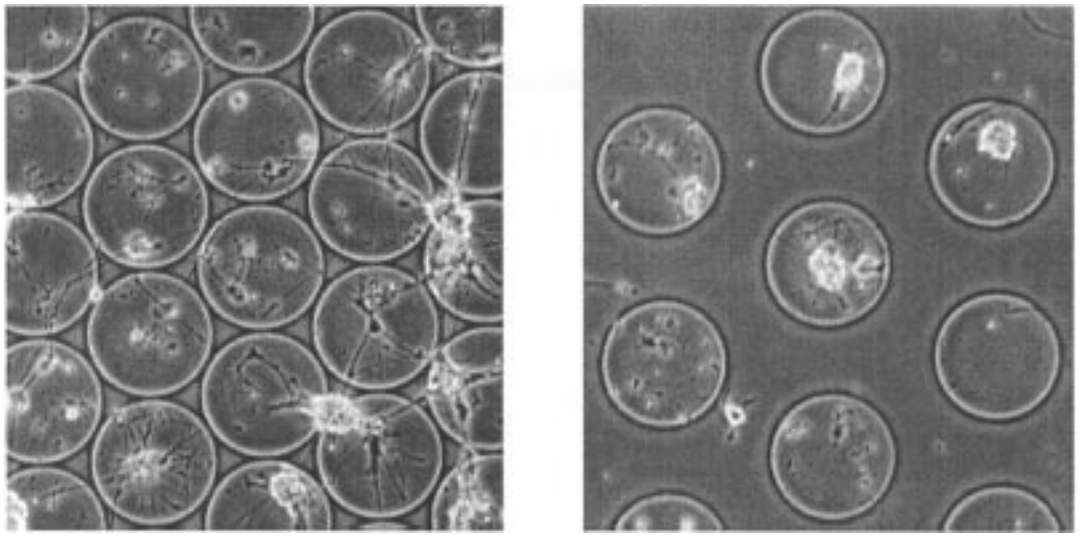

(a) (b)

Fig. 18. Examples of cortical neuron aggregation and development of interconnecting neurite fibers between PEI-coated holes after eight days in vitro on patterned surfaces with typical separation distances of (a) 10 μm and (b) 90μm between the PEI-coated wells. Diameter wells is 150 μm.

as the cumulative fluorescence of red (nonviable) and green (viable) neurons overlapping each other [43]. The yellow color, especially present in neural aggregates, suggests that aggregates are clusters of viable *and* nonviable cells.

Development of connections across the interstitial FC layer between neurons on the PEI-coated wells was investigated. Fig. 18 shows the presence of neurite fascicles between PEI-coated wells on 10- and 90-μm separated wells. Quantitative results for experiments with varying separation distance (left) and combined variation (miniaturization) of separation distance/well diameter (right) are summarized in Fig. 19. The results in Fig. 19 demonstrate that interconnecting neurite bundles between PEI-coated wells were especially present on a pattern with a minimal distance of 10 μm between the wells (Fig. 19, left side). The average number of connected wells through neural tissue was 2.2 after eight days and did not approach the maximal number of six. The conclusion is that the CHF_3 plasma deposited FC layer is a nonadhesive surface for cortical neurons and additionally serves as a barrier for developing neurites if the separation distance between the wells is sufficient. The miniaturization experiments (Fig. 19, right) also stressed the importance of a sufficient separation distance between the wells but in addition demonstrated the importance of well diameter. Miniaturization of PEI-coated wells is inevitably accompanied by a decrease in the number of adhering neurons per well. A decreasing number of neural connections between wells could therefore be expected on basis of this principle alone. As the number of connections is positively influenced by the decreasing distance between the wells, the total expected outcome is a moderate increase of neural connections, Nc, through miniaturization. The experiments confirm this expected outcome. The requested state of total isolated networks of neurons on MEAs is easier approached with the miniaturization experiment (lower Nc in general) and offers the extra option to assemble more electrodes on each MEA. However optimal isolation of neurons and neurites into neurophilic PEI-coated holes is still obtained on patterns with large separation distances between the neurophilic PEI-coated wells.

In conclusion, selective adhesion of neurons and subsequent isolation of cortical neurites and/or fasciculated neurites into PEI-coated wells is obtained on wells with a diameter of 150 μm and a separation distance of 90 μm between the wells.

V. Collateral Growth and Guidance

Once long-term cultures of neural clusters on the multielectrode arrays are established, they will have to be connected to spinal motoneurons through axon collaterals. The collaterals will then have to be guided toward, distributed across, and synapsed with the cultured neural clusters. Though by no means trivial, the latter three tasks seem to be easiest. Effective artificial nerve guides will become available in the near future [44]–[46], and these will be used to guide the bundle of collaterals from the peripheral nerve toward the culture chamber. Meanwhile, peripheral nerve transplants may be used, though at the cost of some morbidity to the patient [47], [48]. Gradients of appropriate trophic and tropic factors, and/or grids of adhesive substances can be established across the culture chamber, to distribute the collaterals across the cultured clusters. Synaptogenesis is expected to occur spontaneously upon contact between collateral and cultured neuron.

The collaterals, however, must be induced from adult myelinated peripheral nerves, preferably without damage to the nerve. We will briefly review the process of collateralization during normal development, to establish the potential strategies for collateral induction.

During neural development in general, two kinds of collateralization are recognized; bifurcation and collateral sprouting. In bifurcation, the growth cone at the tip of the

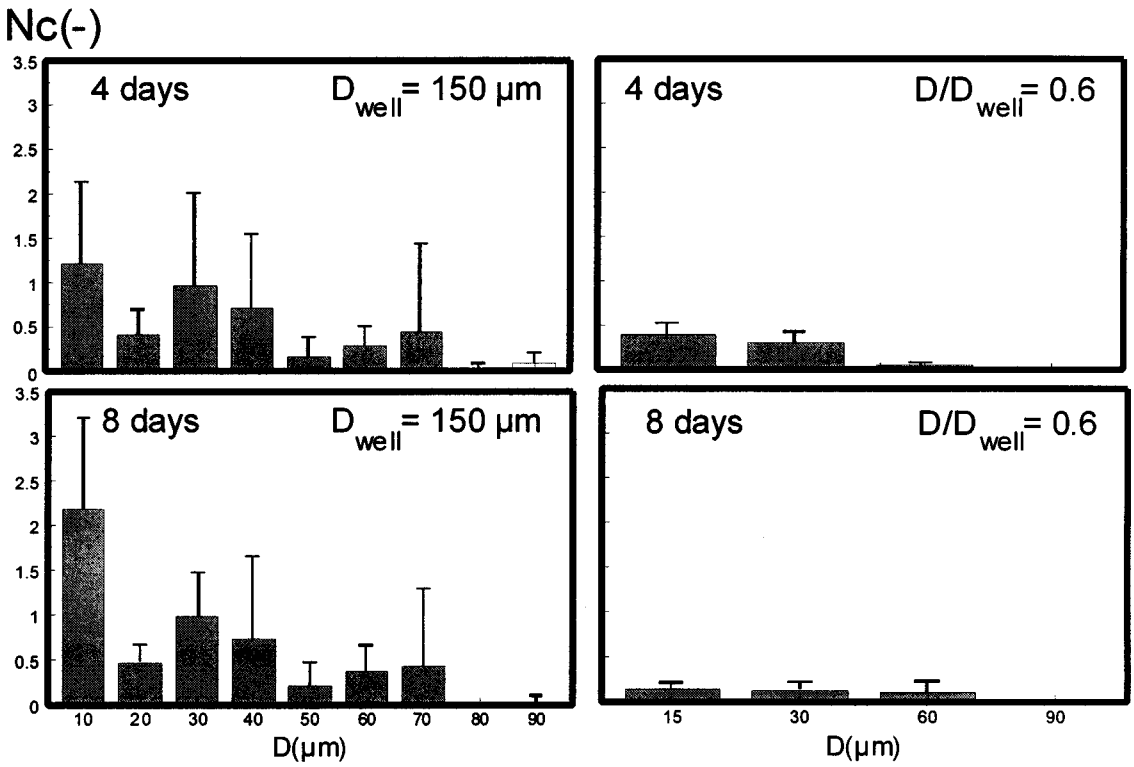

Fig. 19. Average number of connections, Nc, of the PEI-coated well with the six surrounding wells versus the separation distance D between the wells. Connections are formed by neurite fascicles and/or neuron aggregates.

developing axon divides into two or more separate growth cones, each trailing a branch of the axon [49]. The "new" growth cones may proceed along separate paths, or along the same path [50]. Prior to bifurcation, the growth cone usually assumes a more complex shape, i.e., the size of the growth cone and the number of lamelli- and filopodia both increase [51]. The complexity of growth cone shape is related to the number of directional cues in the microenvironment through which the growth cone travels [52], [53]. The potential directional cues are manifold; differential adhesiveness of the substratum [54], [55], local concentration gradients of trophic and tropic factors [56]–[59], growth inhibiting factors [60], [61], growth cone collapsing factors [62], [63], and (weak) electrical fields [64]–[66] have all been implicated in the guidance of growth cone navigation.

In collateral sprouting, a new growth cone emerges from the side of an established (though unmyelinated) axon, distant from the tip of the axon. Collateral sprouts emerge at a more or less perpendicular angle to the original axon, and often continue along a straight course toward a target in their vicinity [67], [68]. It is not clear how collateral sprouts are induced *in vivo*, especially not whether the location of the collateral is determined by the original growth cone as it passes the location of the future sprout, or whether collateral sprouts can be induced arbitrarily along the entire length of the axon [69]. *In vitro* collateral sprouts can be induced by sprouting factors, by nerve growth factor [70], and by the application of relatively strong electrical fields [71], [72].

Motoneurons display yet another type of collateralization; intramuscular terminal sprouting [73], [74]. Motoneuron axons invading developing muscle sprout multiple branches that contact the myotubes and form the motor end plate [75]. This type of sprouting is induced by a muscle derived signal [76], [77], though neonatal Schwann cells can also induce terminal sprouting in motoneurons [78].

During development, thus, a plethora of stimuli may be applied to the outgrowing axon-growth cone unit to induce collaterals of various types. In the adult nervous system, however, the axon is much less inclined toward collateralization (and growth cones, of course, are absent), largely due to the ubiquitous presence of myelin, astrocytes, and Schwann cells [79], [80]. Myelin contains inhibitors of axonal growth and collateralization like myelin associated glycoprotein [81]. Crushing a nerve will stimulate collateral sprouting proximal to the crush site [82], by inducing the local Schwann cells to down-regulate their expression of myelin proteins, and to up-regulate the expression of a series of adhesion molecules that promote growth and collateralization [83], and by up-regulating GAP43 and calcitonin gene-related peptide in the damaged motoneurons [84]. Likewise, partial denervation or paralysis with botulinum toxin of a muscle will induce renewed terminal sprouting from the remaining motoneuron axons [85]–[87], and such sprouting can be enhanced by treatment with gangliosides [88]. Spontaneous sprouting at the neuromuscular junction may be induced by the overexpression of GAP43 in the motoneuron axons [89], and by the local application of insulin-like growth factors [90], [91], and of ciliary neurotrophic factor and basic fibroblast growth factor [92]. All these strategies, however, are not applicable to the present case. While it is possible to induce

terminal sprouting in the muscle without causing damage to the motor unit, the induced sprouts will remain within the muscle. To induce collateral sprouting from the peripheral nerve, the nerve apparently has to be damaged (transected, crushed, or constricted).

Yet, there might be an approach that will result in collateral branching, without damage to the peripheral axons. Lundborg and coworkers transected, in rats, the proximal peroneal fascicle supplying the tibialis anterior muscle. Following a seven-day predegeneration period the distal stump was sutured end-to-side to the ipsilateral tibial fascicle. After 90 days substantial contraction in both the native gastrocnemius muscle and the foreign tibialis anterior muscle followed stimulation of the tibial nerve proximal to the anastomosis [93]. In a similar study, Chen and Brushart demonstrated that the transplantation of denervated muscle and Schwann cells around a perineurial window promotes motor and sensory nerve collateral sprouting into a peripheral nerve anastomosed to this window [94]. These studies suggest that collateral sprouting may occur from intact axons through a perineurial window, upon stimulation of the axon shafts with signals from denervated Schwann and muscle cells. It will, thus, be possible to induce a collateral branch by anastomosing an artificial biodegradable nerve guide loaded with Schwann cells [95] and the appropriate motoneurotrophins onto a lateral perineurial window in a peripheral nerve. Though autologous Schwann cells are the most advantageous with respect to collateralization and outgrowth [95], their harvesting implies at least the dissection of a peripheral nerve. Heterologous Schwann cells multiplied and preconditioned in culture may also be used [96], [97], eventually these will be replaced by autologous Schwann cells migrating into the graft [98], [99]. At present part of our research is aimed at the development of such an artificial biodegradable nerve graft, to be employed both as a conduit for the guidance of induced collaterals toward a cultured probe, and as a conduit for regenerating nerves.

A. Experiments

To distribute afferent collaterals among the cultured neural clusters, we cultured spinal cord explants according to a previously described protocol [100] on coverslips printed with a micropatterned grid of poly (ethylene imine) (PEI) lines. The grid was prepared by microcontact printing with silicone stamps (courtesy Martin Stelzle, NMI Reutlingen Germany), featuring ridges 75 μm wide and 25 μm high, intersecting perpendicular at 325 μm intervals.

The stamps were made (temporarily) hydrophilic by argon plasma cleaning (Biorad sputter coater, 3 min at 2.5 kV), and stored. Immediately prior to printing, a stamp was wetted with PEI (0.2 mg/ml) for 1 min, then dried with filtered pulsed air. The stamp was then arranged onto the coverslip and manual pressure was applied. Equal application of pressure was observed with an inverted microscope, allowing illumination and observation from below, through the to-be-printed coverslip. Pressure was maintained for 1 min. Transferred PEI can be observed by transillumination with an inverted microscope at high magnification.

A bunch of a few glass fibers was deposited on the coverslip, and one extremity of the bunch was fixed in place with a drop of collagen solution [100]. The coverslip was placed into a petri dish and stored in a CO_2 incubator (37 °C, 5.5% CO_2) for 2 h, to achieve gelation of the collagen. After this period, 1 ml of culture medium (R_{12}) [101] was added to the petri dish.

All procedures involving the husbandry, handling, and sacrifice of experimental animals were performed in accordance with the protocol approved by our institutional animal care committee (UDEC 97 035), and in accordance with national laws. Wistar Albino Glaxo rat neonates sacrificed during the first day of life were used.

All procedures for the preparation of spinal and cortical explants took place under antiseptic conditions. The rat was introduced into the laminar flow cabinet, submerged into 70% ethanol, rinsed in cold normal saline and decapitated immediately. Under a dissecting microscope, the lower spinal cord was exposed by laminectomy. A longitudinal cut in the meninges was extended all along the exposed spinal cord, all spinal nerves were transected, and the exposed cord was excised. This portion was collected in a R_{12} culture medium and the meningial coverings were stripped away. The lumbar enlargement was resected and chopped immediately into 250 μm slices using a tissue chopper. These slices were collected in the same medium and separated by gentle aspirations with a Pasteur pipette. Taking advantage of the tendency of the cord to split along the median, the slices were separated into lateral halves. For culturing a selection of the resulting slices (explants) was made based on appearance (undamaged), thickness (uniform), and absence of meningial covering.

Each selected explant was placed on a pretreated (see above) coverslip (in a petri dish) and secured with the glass fibers. The petri dish again stored in the CO_2 incubator. The culture medium was refreshed every other day. Cultures were maintained for six days. Outgrowth from the explant was observed using phase contrast microscopy.

Axons emerged randomly from the explants (Fig. 20), but upon crossing one of the grid lanes they subsequently followed the grid pattern. Axon bundles were segregated along the side of the grid lanes, presumably growing along the most concentrated sites of PEI deposition. After six days in culture, the bundles of axons reached a length of up to 2400 μm. The outgrowing axon bundles tended to distribute themselves across the grid pattern, by branching or subdivision into smaller bundles at the intersections, progressively occupying the available grid lines while growing outward from the explant.

Superimposing a PEI grid pattern upon the surface of the microelectrode array, prior to seeding of the neurons, appears to be a suitable method to distribute afferent collaterals among the cultured neurons. Future experiments will determine whether the PEI grid persists sufficiently long, as there will necessarily be a substantial delay between the initiation of the neural culture on the microelectrode array, and the ingrowth of the axon collaterals.

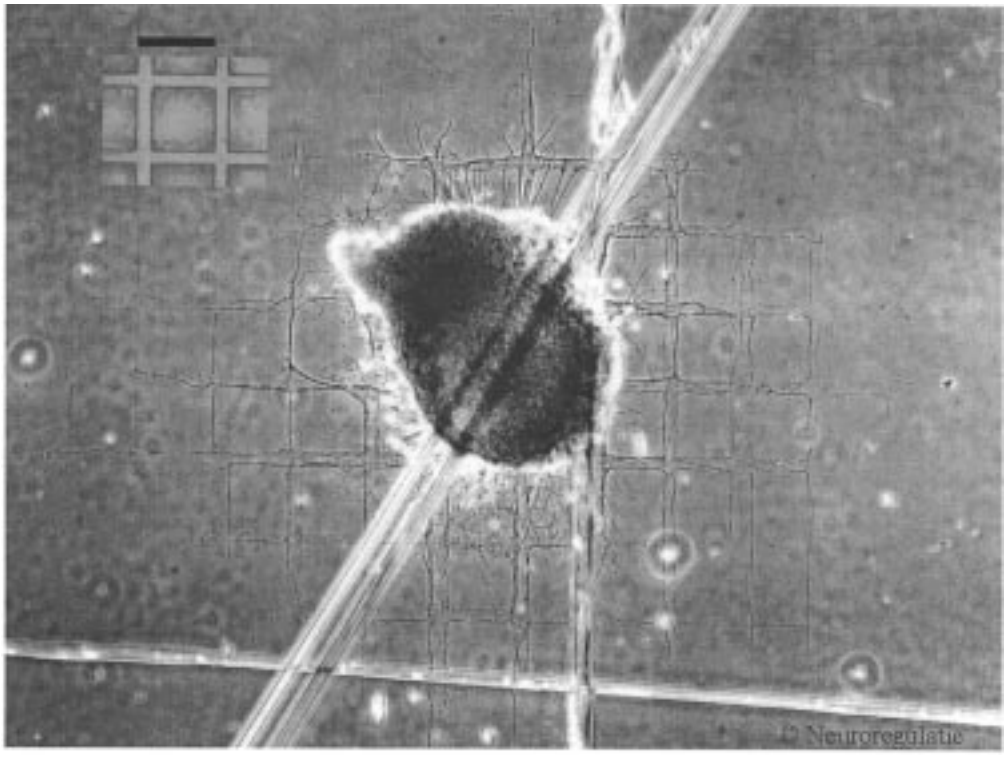

Fig. 20. Outgrowth from a neonatal rat lumbar spinal cord explant, after six days in culture. Two glass fibers (oblique linear structure) overlying the explant immobilize it against the coverslip. The two perpendicular lines are scratches made with a diamond pen on the opposite side of the coverslip; these are used to align the stamped pattern and the tissue upon explantation. In the upper left corner, a photograph of a part of the stamp is superimposed on the grid. Phase contrast microscopy, six days in culture, bar 400 μm.

Incidentally, the same experimental paradigm (explant culture on patterned substrates on microelectrode arrays) is ideally suitable for the study of collateral induction through electrical stimulation [71]. These studies are currently in progress. Finally, explants cultured on superimposed patterns of different adhesive substances may be employed to obtain even more intricate and coordinated networks of axons *in vitro*.

VI. Conclusion and Outlook

Neural and cellular engineering combine neuroscience, microtechnology, electrophysiology, cell culturing and manipulation, electrical modeling and simulation.

Neural and cellular engineering are two relatively new fields of engineering, leading to exciting possibilities to couple the nervous world to the electronic and to develop neural prostheses. It has opened also other (not presented in this paper), promising research areas such as the study and understanding of live neuronal network activity and of elementary "brain" functioning in such networks [102], [103]. It may serve the development of brain interfaces [104] and it is of use for learning and memory in brain-like networks [105].

In this paper, we have illustrated how MEA technology can be advanced into a useful tool for neuroelectronic interfacing. The development toward implantable cultured neural probes may become very beneficial for restoration of disabled neural functions. The basic requirements for a selective and efficient coupling between electrodes and neurites seem to be fulfilled with success. These are: 1) MEA technology enables microelectrodes to be patterned and embedded in flat substrates in large quantities and at the scale of neural dimensions; 2) substrates can be chemically modified for local adhesion of cultured neuronal cells, centered around electrode sites; 3) dissociated neuronal cells can be trapped, adhered and sealed onto neurophilic areas on the substrate; and 4) collateral sprouts can be evoked form spinal cord explants and guided along neurophilic paths over substrates.

For practical future use in humans, first another number of essential steps have to be taken such as: 5) assembly and miniaturization; 6) implantation in animal; 7) testing whether high selectivity and efficiency can be reached in a live implant in the ventral horn area; and 8) biocompatibility and long-term acceptance and survival. Our current and future research is focused on these latter issues.

References

[1] R. S. Tyler, Ed., *Cochlear implants, Audiological Foundations.* San Diego, CA: Singular Publishing Group, 1993.

[2] S. Parrini, J. Delbeke, V. Legat, and C. Veraart, "Modeling analysis of human optic nerve fiber excitation based on experimental data'," *Med. Biol. Eng. Comput.*, vol. 38, pp. 454–464, 2000.

[3] J. P. A. Smit, W. L. C. Rutten, and H. B. K. Boom, "Endoneural selective stimulation using wire microelectrode arrays," *IEEE Trans. Rehab. Eng.*, vol. 7, pp. 399–412, 1999.

[4] W. L. C. Rutten and J. P. A. Smit, "Efficiency of endoneural stimulation with 5- to 24-fold microelectrode arrays," in *Proc. 20th Annu. Int. Conf. IEEE Engineering in Medicine and Biology Society*, Hong Kong, 1998, p. 4.
[5] W. L. C. Rutten, J. P. A. Smit, T. A. Frieswijk, J. A. Bielen, A. L. H. Brouwer, J. R. Buitenweg, and T. Heida, "Neuro-electronic interfacing with multi electrode arrays ; Selectivity and efficiency of motor-fiber stimulation," *IEEE Eng. Med. Biol. Mag.*, vol. 18/3, pp. 47–55, 1999.
[6] W. L. C. Rutten, "Neurotechnology," in *Encyclopedia of Electrical and Electronics Engineering*, J. G. Webster, Ed. New York: Wiley, 1999, vol. 14, Ed, pp. 366–373.
[7] W. L. C. Rutten, H. van Wier, and J. H. M. Put, "Sensitivity and selectivity of intraneural stimulation using a silicon electrode array," *IEEE Trans. Biomed. Eng.*, vol. 38, pp. 192–198, 1991.
[8] W. L. C. Rutten and J. H. Meier, "Selectivity of intraneural prosthetic interfaces for muscular control," *Med. Biol. Eng. Comput.*, vol. 29, pp. NS3–NS7, 1991.
[9] J. H. Meier, W. L. C. Rutten, and H. B. K. Boom, "Force recruitment during electrical nerve stimulation with multipolar intrafascicular electrodes," *Med. Biol. Eng. Comput.*, vol. 33, pp. 409–417, 1995.
[10] K. Yoshida and K. Horch, "Closed-loop control of ankle position using muscle afferent feedback with functional neuromuscular stimulation," *IEEE Trans. Biomed. Eng.*, vol. 43, pp. 167–176, 1996.
[11] J. A. Bielen, A. Schmidt, R. Weiel, and W. L. C. Rutten, "Fabrication of multi electrode array structures for intra-neural stimulation: assessment of the LIGA method," in *Proc. 18th Int. Conf. Engineering in Medicine and Biology*, Amsterdam, The Netherlands, 1996, p. 2.
[12] Q. Bai, K. D. Wise, and D. J. Anderson, "A high-yield microassembly structure for three-dimensional microelectrode arrays," *IEEE Trans. Biomed. Eng.*, vol. 47, pp. 281–289, 2000.
[13] D. J. Edell, "A peripheral nerve information transducer for amputees: long-term multichannel recordings from rabbit peripheral nerves," *IEEE Trans. Biomed. Eng.*, vol. 33, pp. 203–214, 1986.
[14] G. T. A. Kovacs, C. W. Storment, M. Halks-Miller, C. R. Belczynski, C. C. Della Santina, E. R. Lewis, and N. I. Maluf, "Silicon-substrate micro-electrode arrays for parallel recording of neural activity in peripheral and cranial nerves," *IEEE Trans. Biomed. Eng.*, vol. 41, pp. 567–577, 1994.
[15] T. Laurell, J. Drott, Q. Zhao, L. Wallman, and L. Montelius *et al.*, "Perforated silicon membranes as an artificial neural contact pad—chip design and tissue implant response," in *Proc 18th Int. Conf. Engineering in Medicine and Biology*, Amsterdam, The Netherlands, p. 2.
[16] W. G. Regehr, J. Pine, C. S. Cohan, M. D. Mischke, and D. W. Tank, "Sealing cultured invertebrate neurons to embedded dish electrodes facilitates long-term electrical stimulation and recording," *J. Neurosci. Meth.*, vol. 30, pp. 91–106, 1989.
[17] L. J. Breckenridge, R. J. A. Wilson, P. Connolly, A. S. G. Curtis, J. A. T. Dow, S. E. Blackshaw, and C. D. W. Wilkinson, "Advantages of using microfabricated extracellular electrodes for in vitro neuronal recording," *J. Neurosci.*, vol. 42, pp. 266–276, 1995.
[18] M. Bove, M. Grattarola, S. Martinoia, and G. Verreschi, "Interfacing cultured neurons to planar substrate microelectrodes: characterization of the neuron-to-microelectrode junction," *Bioelectrochem. Bioenergetics*, vol. 38, pp. 255–265, 1995.
[19] J. R. Buitenweg, W. L. C. Rutten, and E. Marani, "Finite element modeling of the neuron–electrode interface: Stimulus transfer and geometry," in *Proc. 1st Joint BMES/EMBS Conf.*, 1999.
[20] ——, "Geometry based dynamic modeling of the neuron–electrode interface," presented at the World Congr. Medical Physics and Biomedical Engineering, Chicago, IL, 2000.
[21] J. R. Buitenweg, W. L. C. Rutten, W. P. A. Willems, and J. W. van Nieuwkasteele, "Measurement of sealing resistance of cell-electrode interfaces in neuronal cultures using impedance spectroscopy," *Med. Biol. Eng. Comp.*, vol. 36, pp. 630–637, 1998.
[22] A. H. Pohl, "Some effects of nonuniform fields on dielectrics," *J. Appl. Phys.*, vol. 29, pp. 1182–1189, 1958.
[23] ——, *Dielectrophoresis*. London, U.K.: Cambridge Univ. Press, 1978.
[24] G. Fuhr, H. Glasser, T. Müller, and Th. Schnelle, "Cell manipulation and cultivation under AC electric field influence in highly conductive culture media," *Biochim. Biophys. Acta*, vol. 1201, pp. 353–360, 1994.
[25] G. Fuhr and S. G. Shirley, "Cell handling and characterization using micron and submicron electrode arrays: state of the art and perspectives of semiconductor microtools," *J. Micromech. Microeng.*, vol. 5, pp. 77–85, 1995.
[26] N. G. Green and H. Morgan, "Dielectrophoretic separation of nanoparticles," *J. Phys. D: Appl. Phys.*, vol. 30, pp. L41–L44, 1997.
[27] H. Morgan, M. P. Hughes, and N. G. Green, "Separation of submicron bioparticles by dielectrophoresis," *Biophys. J.*, vol. 77, pp. 516–525, 1999.
[28] A. Irimajiri, K. Asami, T. Ichinowatari, and Y. Kinoshita, "Passive electrical properties of the membrane and cytoplasm of cultured rat basophil leukemia cells: I. Dielectric behavior of cell suspensions in 0.01–500 MHz and its simulation with a single-shell model," *Biochim. Biophys. Acta*, vol. 896, pp. 203–213, 1987.
[29] J. J. Zielinski, P. Marszalek, and M. Fikus, "A new method for the investigation of cellular dielectrophoresis," *Z. Naturforsch.*, vol. 44c, pp. 845–848, 1989.
[30] K. V. I. S. Kaler and T. B. Jones, "Dielectrophoretic spectra of single cells determined by feedback-controlled levitation," *Biophys. J.*, vol. 57, pp. 173–182, 1990.
[31] T. Müller, A. Gerardino, Th. Schnelle, S. G. Shirley, F. Bordoni, G. De Gasperis, R. Leoni, and G. Fuhr, "Trapping of micrometer and sub-micrometer particles by high-frequency electric fields and hydrodynamic forces," *J. Phys. D: Appl. Phys.*, vol. 29, pp. 340–349, 1996.
[32] T. Schnelle, T. Müller, S. Fiedler, S. G. Shirley, K. Ludwig, A. Herrmann, G. Fuhr, B. Wagner, and U. Zimmermann, "Trapping of viruses in high-frequency electric field cages," *Naturwissenschaften*, vol. 83, pp. 172–176, 1996.
[33] U. Zimmermann and G. A. Neil, *Electromanipulation of Cells*. Boca Raton, Florida: CRC, 1996.
[34] D. Kleinfeld, K. H. Kahler, and P. E. Hockberger, "Controlled outgrowth of dissociated neurons on patterned substrates," *J. Neurosci.*, vol. 8, pp. 4098–4120, 1988.
[35] J. M. Corey, B. C. Wheeler, and G. J. Brewer, "Micrometerresolution silane-based patterning of hippocampal neurons: critical variables in photoresist and laser ablation processes for substrate fabrication," *IEEE Trans. Biomed. Eng.*, vol. 43, pp. 944–955, 1996.
[36] S. A. Makohliso, L. Giovangrandi, D. Leonard, H. J. Mathieu, M. Ilegems, and P. Aebisher, "Application of Teflon-AF® thin films for bio-patterning of neural cell adhesion," *Biosens. Bioelectr.*, vol. 13, pp. 1227–1235, 1998.
[37] H. V. Jansen, J. G. E. Gardeniers, J. Elders, H. A. C. Tilmans, and M. Elwenspoek, "Applications of fluorocarbon polymers in micromechanics and micromachining," *Sens. Actuators A*, vol. 41–42, pp. 136–140, 1994.
[38] H. V. Jansen, "Plasma etching in microtechnology," Ph.D. dissertation, Univ. Twente, The Netherlands, 1996.
[39] J. M. Schakenraad, J. H. Kuit, J. Arends, H. J. Busscher, J. Feijen, and C. R. H. Wildevuur, "In vivo quantification of cell-polymer interactions," *Biomaterials*, vol. 8, pp. 207–210, 1987.
[40] U. T. Rüegg and F. Hefti, "Growth of dissociated neurons in culture dishes coated with synthetic polymeric amines," *Neurosci. Lett.*, vol. 49, pp. 319–324, 1984.
[41] I. H. Lelong, V. Petegnief, and G. Rebel, "Neuronal cells mature faster on polyethylenimine coated plates than on polylysine coated plates," *J. Neurosci. Res.*, vol. 32, pp. 562–569, 1992.
[42] T. G. Ruardij, M. H. Goedbloed, and W. L. C. Rutten, "Adhesion and patterning of cortical neurons on polyethylenimine and fluorocarbon-coated surfaces," IEEE Trans. Biomed. Eng., to be published.
[43] H. L. Bank, "Rapid assessment of islet viability with acridine orange and propidium iodide," *In Vitro Cell. Dev. Biol.*, vol. 24, pp. 266–273, 1988.
[44] V. B. Doolabh, M. C. Hertl, and S. E. Mackinnon, "The role of conduits in nerve repair: a review," *Rev. Neurosci.*, vol. 7, pp. 47–84, 1996.
[45] T. Hadlock, J. Elisseeff, R. Langer, J. Vacanti, and M. Cheney, "A tissue-engineered conduit for peripheral nerve repair," *Arch. Otolaryngology Head Neck Surg.*, vol. 124, pp. 1081–1086, 1998.
[46] M. F. Meek, J. R. Dijkstra, W. F. Den Dunnen, P. J. Ijkema, J. M. Schakenraad, A. Gramsbergen, and P. H. Robinson, "Functional assessment of sciatic nerve reconstruction: Biodegradable poly (DLLA-epsilon-CL) nerve guides versus autologous nerve grafts," *Microsurgery*, vol. 19, pp. 381–388, 1999.
[47] R. T. Thomeer and M. J. Malessy, "Surgical repair of brachial plexus injury," *Clin. Neurol. Neurosurg.*, vol. 95, pp. S65–S72, 1993.

[48] C. A. Holtzer, H. K. Feirabend, E. Marani, and R. T. Thomeer, "Ultrastructural and quantitative motoneuronal changes after ventral root avulsion favor early surgical repair," *Arch. Physiol. Biochem.*, vol. 108, pp. 293–309, 2000.
[49] M. Hollyday and M. Morgancarr, "Chick wing innervation .2. Morphology of motor and sensory axons and their growth cones during early development," *J. Comp. Neurol.*, vol. 357, pp. 254–271, 1995.
[50] D. D. O'Leary, A. R. Bicknese, J. A. de-Carlos, C. D. Heffner, S. E. Koester, L. J. Kutka, and T. Terashima, "Target selection by cortical axons: alternative mechanisms to establish axonal connections in the developing brain," in *Cold Spring Harbor Symp. Quant. Biol.*, vol. 55, 1990, pp. 453–468.
[51] M. J. Ferns and M. Hollyday, "Chick wing innervation .3. Formation of axon collaterals in developing peripheral nerves," *J. Comp. Neurol.*, vol. 357, pp. 272–280, 1995.
[52] P. Bovolenta and A. Mason, "Growth cone morphology varies with position in the developing mouse visual pathway from retina to first targets," *J. Neurosci.*, vol. 7, pp. 1447–1460, 1987.
[53] P. Bovolenta and J. Dodd, "Guidance of commissural growth cones at the floor plate in embryonic rat spinal cord," *Development*, vol. 109, pp. 435–447, 1990.
[54] U. S. Rutishauser, "Influences of the neural cell adhesion molecule on axon growth and guidance," *J. Neurosci. Res.*, vol. 13, pp. 123–131, 1985.
[55] P. Pesheva, S. Kuklinski, B. Schmitz, and R. Probstmeier, "Galectin-3 promotes neural cell adhesion and neurite growth," *J. Neurosci. Res.*, vol. 54, pp. 639–654, 1998.
[56] A. G. Lumsden and A. M. Davies, "Chemotropic effect of specific target epithelium in the developing mammalian nervous system," *Nature*, vol. 323, pp. 538–539, 1986.
[57] N. L. Perez, M. A. Sosa, and D. P. Kuffler, "Growth cones turn up concentration gradients of diffusible peripheral target-derived factors," *Exp. Neurol.*, vol. 145, pp. 196–202, 1997.
[58] M. Tessier-Lavigne, "Axon guidance by diffusible repellants and attractants," *Current Opin. Genetics Dev.*, vol. 4, pp. 596–601, 1994.
[59] E. A. Lakke, "Neurotropic attraction: Facts and fiction," *Biomed. Rev.*, vol. 4, pp. 95–102, 1995.
[60] S. Guthrie and A. Pini, "Chemorepulsion of developing motor axons by the floor plate," *Neuron*, vol. 14, pp. 1117–1130, 1995.
[61] B. J. Fredette, J. Miller, and B. Ranscht, "Inhibition of motor axon growth by T-cadherin substrata," *Development*, vol. 122, pp. 3163–3171, 1996.
[62] J. Fan and J. A. Raper, "Localized collapsing cues can steer growth cones without inducing their full collapse," *Neuron*, vol. 14, pp. 263–274, 1995.
[63] M. Placzek, M. Tessier-Lavigne, T. Yamada, J. Dodd, and T. M. Jessell, "Guidance of developing axons by diffusible chemoattractants," *Cold Spring Harbor Symp. Quant. Biol*, vol. 55, pp. 279–289, 1990.
[64] C. D. McCaig, "Electric fields, contact guidance and the direction of nerve growth," *J. Embryol. Exp. Morphol.*, vol. 94, pp. 245–255, 1986.
[65] L. Erskine, R. Stewart, and C. D. McCaig, "Electric field-directed growth and branching of cultured frog nerves: Effects of aminoglycosides and polycations," *J. Neurobiol.*, vol. 26, pp. 523–536, 1995.
[66] A. M. Rajnicek, K. R. Robinson, and C. D. McCaig, "The direction of neurite growth in a weak DC electric field depends on the substratum: contributions of adhesivity and net surface charge," *Dev. Biol.*, vol. 203, pp. 412–423, 1998.
[67] D. D. O'Leary and T. Terashima, "Cortical axons branch to multiple subcortical targets by interstitial axon budding: implications for target recognition and waiting periods," *Neuron*, vol. 1, pp. 901–910, 1988.
[68] C. D. Heffner, A. G. Lumsden, and D. D. O'Leary, "Target control of collateral extension and directional axon growth in the mammalian brain," *Science*, vol. 247, pp. 217–220, 1990.
[69] M. Bastmeyer, M. M. Daston, H. Possel, and D. D. O'Leary, "Collateral branch formation related to cellular structures in the axon tract during corticopontine target recognition," *J. Comp. Neurol.*, vol. 392, pp. 1–18, 1998.
[70] G. Gallo and P. C. Letourneau, "Localized sources of neurotrophins initiate axon collateral sprouting," *J. Neurosci.*, vol. 18, pp. 5403–5414, 1998.
[71] C. D. McCaig, "Nerve branching is induced and oriented by a small applied electric field," *J. Cell Sci.*, vol. 95, pp. 605–615, 1990.
[72] C. D. McCaig, L. Sangster, and R. Stewart, "Neurotrophins enhance electric field-directed growth cone guidance and directed nerve branching," *Dev. Dynamics*, vol. 217, pp. 299–308, 2000.
[73] W. B. Gan and J. W. Lichtman, "Synaptic segregation at the developing neuromuscular junction," *Science*, vol. 282, pp. 1508–1511, 1998.
[74] J. P. Fraher, G. F. Kaar, D. C. Bristol, and J. P. Rossiter, "Development of ventral spinal motoneurone fibers: a correlative study of the growth and maturation of central and peripheral segments of large and small fiber classes," *Progr. Neurobiol.*, vol. 31, pp. 199–239, 1988.
[75] T. Meier and B. G. Wallace, "Formation of the neuromuscular junction: molecules and mechanisms," *Bioessays*, vol. 20, pp. 819–829, 1998.
[76] R. G. Smith and S. H. Appel, "Extracts of skeletal muscle increase neurite outgrowth and cholinergic activity of fetal rat spinal motor neurons," *Science*, vol. 219, pp. 1079–1081, 1983.
[77] S. Rotshenker, G. Ring, M. Tal, H. Sugarman, and F. Reichert, "Regulation of motor axon sprouting," *Isr. J. Med. Sci.*, vol. 23, pp. 89–94, 1987.
[78] M. A. Hill, "The growth of motoneurones and their neurites in relation to Schwann cells harvested from sciatic nerve," *Brain Res.*, vol. 430, pp. 243–253, 1987.
[79] C. Bandtlow, T. Zachleder, and M. E. Schwab, "Oligodendrocytes arrest neurite growth by contact inhibition," *J. Neurosci.*, vol. 10, pp. 3837–3848, 1990.
[80] E. Benavides and J. Alvarez, "Peripheral axons of Wld(s) mice, which regenerate after a delay of several weeks, do so readily when transcription is inhibited in the distal stump," *Neurosci. Lett.*, vol. 258, pp. 77–80, 1998.
[81] Y. J. Shen, M. E. DeBellard, J. L. Salzer, J. Roder, and M. T. Filbin, "Myelin-associated glycoprotein in myelin and expressed by Schwann cells inhibits axonal regeneration and branching," *Molec. Cell. Neurosci.*, vol. 12, pp. 79–91, 1998.
[82] T. M. Brushart, J. G. a. Kessens, Y. G. Chen, and R. M. Royall, "Contributions of pathway and neuron to preferential motor reinnervation," *J. Neurosci.*, vol. 18, pp. 8674–8681, 1998.
[83] J. L. Bixby, J. Lilien, and L. F. Reichardt, "Identification of the major proteins that promote neuronal process outgrowth on Schwann cells in vitro," *J. Cell Biol.*, vol. 107, pp. 353–361, 1988.
[84] F. Piehl, H. Hammarberg, T. Hokfelt, and S. Cullheim, "Regulatory effects of trophic factors on expression and distribution of CGRP and GAP-43 in rat motoneurons," *J. Neurosci. Res.*, vol. 51, pp. 1–14, 1998.
[85] J. R. Slack, W. G. Hopkins, and M. N. Williams, "Nerve sheaths and motoneurone collateral sprouting," *Nature*, vol. 282, pp. 506–507, 1979.
[86] W. G. Hopkins, M. C. Brown, and R. J. Keynes, "Nerve growth from nodes of Ranvier in inactive muscle," *Brain Res.*, vol. 222, pp. 125–128, 1981.
[87] H. Li, C. Wigley, and S. M. Hall, "Chronically denervated rat Schwann cells respond to GGF in vitro," *Glia*, vol. 24, pp. 290–303, 1998.
[88] A. Gorio, P. Marini, and R. Zanoni, "Muscle reinnervation–III. Motoneuron sprouting capacity, enhancement by exogenous gangliosides," *Neuroscience*, vol. 8, pp. 417–429, 1983.
[89] L. Aigner, S. Arber, J. P. Kapfhammer, T. Laux, C. Schneider, F. Botteri, H. R. Brenner, and P. Caroni, "Overexpression of the neural growth-associated protein GAP-43 induces nerve sprouting in the adult nervous system of transgenic mice," *J. Anatomy*, vol. 83, pp. 269–278, 1995.
[90] N. T. Neff, D. Prevette, L. J. Houenou, M. E. Lewis, M. A. Glicksman, Q. W. Yin, and R. W. Oppenheim, "Insulin-like growth factors: putative muscle-derived trophic agents that promote motoneuron survival," *J. Neurobiol.*, vol. 24, pp. 1578–1588, 1993.
[91] P. Caroni, C. Schneider, M. C. Kiefer, and J. Zapf, "Role of muscle insulin-like growth factors in nerve sprouting: suppression of terminal sprouting in paralyzed muscle by IGF-binding protein 4," *J. Cell Biol.*, vol. 125, pp. 893–902, 1994.
[92] M. E. Gurney, H. Yamamoto, and Y. Kwon, "Induction of motor neuron sprouting in vivo by ciliary neurotrophic factor and basic fibroblast growth factor," *J. Neurosci.*, vol. 12, pp. 3241–3247, 1992.
[93] G. Lundborg, Q. Zhao, M. Kanje, N. Danielsen, and J. M. Kerns, "Can sensory and motor collateral sprouting be induced from intact peripheral nerve by end-to-side anastomosis?," *J. Hand Surg. Br.*, vol. 19, pp. 277–282, 1994.
[94] Y. G. Chen and T. M. Brushart, "The effect of denervated muscle and Schwann cells on axon collateral sprouting," *J. Hand Surg. Amer.*, vol. 23A, pp. 1025–1033, 1998.
[95] F. J. Rodriguez, E. Verdu, D. Ceballos, and X. Navarro, "Nerve guides seeded with autologous schwann cells improve nerve regeneration," *Exp. Neurol.*, vol. 161, pp. 571–584, 2000.

[96] V. Guenard, N. Kleitman, T. K. Morrissey, R. P. Bunge, and P. Aebischer, "Syngeneic Schwann cells derived from adult nerves seeded in semipermeable guidance channels enhance peripheral nerve regeneration," *J. Neurosci.*, vol. 12, pp. 3310–3320, 1992.

[97] E. Spierings, C. L. Vleggeert-Lankamp, E. Marani, R. T. Thomeer, and T. H. Ottenhoff, "Allorecognition of artificial nerve guides filled with human Schwann cells: an in vitro pilot study," *Transplantation*, vol. 69, pp. 455–456, 2000.

[98] D. A. Abernethy, P. K. Thomas, A. Rud, and R. H. King, "Mutual attraction between emigrant cells from transected denervated nerve," *J. Anatomy*, vol. 184, pp. 239–249, 1994.

[99] K. Katsube, K. Doi, T. Fukumoto, Y. Fujikura, M. Shigetomi, and S. Kawai, "Successful nerve regeneration and persistence of donor cells after a limited course of immunosuppression in rat peripheral nerve allografts," *Transplantation*, vol. 66, pp. 772–777, 1998.

[100] J. M. P. Mouveroux, M. Verkijk, E. A. J. F. Lakke, and E. Marani, "Intrinsic properties of the developing motor cortex in the rat: in vitro axons from the medial somatomotor cortex grow faster than axons from the lateral somatomotor cortex," *Brain Res. Develop. Brain Res.*, vol. 122, pp. 59–66, 2000.

[101] H. J. Romijn, F. van-Huizen, and P. S. Wolters, "Toward an improved serum-free, chemically defined medium for long-term culturing of cerebral cortex tissue," *Neurosci. Biobehav. Rev.*, vol. 8, pp. 301–334, 1984.

[102] Y. Jimbo, A. Kawana, P. Parodi, and V. Torre, "The dynamics of a neuronal culture of dissociated cortical neurons of neonatal rats," *Biol. Cybern.*, vol. 83, pp. 1–20, 2000.

[103] W. L. C. Rutten, T. G. Ruardij, and J. van Pelt, "Neuronal networks on 'cultured probe' micro electrode arrays: network confinement and activity patterns," in *Proc. Atlantic Symp. Computational Biology and Genome Information Systems and Technology*, Durham, NC, Mar. 15–17, 2001, pp. 101–105.

[104] J. Wessberg, C. R. Stambaugh, J. D. Kralik, P. D. Beck, M. Laubach, J. K. Chapin, J. Kim, S. J. Biggs, A. Srinvasan, and M. A. L. Nicolelis, "Real-time prediction of hand trajectory by ensembles of cortical neurons in primates," *Nature*, vol. 408, pp. 361–365, 2000.

[105] G. Bi and M. Poo, "Distributed synaptic modification in neural networks induced by patterned stimulation," *Nature*, vol. 401, pp. 792–796, 1999.